

Application of the Sono-Fenton Process for Doxycycline Degradation Using Taguchi's Experimental Designs

Nabila Boucherit^{1,2*}, Mohamed Barki³, Achouak Madani², Abdelkarim Brahimi⁴, and Nassiba Mimi¹

¹Department of Material Sciences, Faculty of Sciences, University of Medea, Urban Pole, Medea 26000, Algeria

²Laboratory of BioMaterials and Transport Phenomena, Urban Pole, Medea 26000, Algeria

³University of Tizi Ouzou, Tizi Ouzou 15000, Algeria

⁴El-Birine Research Center (CRNB), COMENA, BP180 Ain Oussera, Djelfa 17000, Algeria

* **Corresponding author:**

email: na_boucherit@yahoo.fr

Received: December 12, 2024

Accepted: August 4, 2025

DOI: 10.22146/ijc.102531

Abstract: This study aimed to evaluate the effectiveness of the sono-Fenton method via the oxidation of a tetracycline antibiotic molecule: doxycycline hyclate (DXC), chosen as a model compound due to its regular detection in wastewater treatment plant effluents. Taguchi's statistical method was applied via the orthogonal and full experimental designs to optimize the influential parameters. The study's results showed that the concentration of the oxidizing agent (H_2O_2) was the most effective factor for DXC degradation. The optimum conditions for antibiotic removal were initial DXC concentration at level 1 (0.5 mg L^{-1}), H_2O_2 concentration at level 2 (1.25 mM), and catalyst concentration at level 2 (0.65 mM). The results showed that the value predicted theoretically and determined via a matrix model for degradation efficiency was confirmed by the experimental value, which deviated by 3.11%. The various products obtained, characterized by UV-vis and HPLC, showed the transformation of DXC molecules by sono-Fenton oxidation.

Keywords: doxycycline; modelling; oxidation; Taguchi; toxicity

■ INTRODUCTION

The production and consumption of antibiotics have increased in recent years, resulting in their permanent presence in liquid effluents and soils, either as parent molecules or in metabolized form [1]. It has been reported that tetracyclines (TCs) are among the most widely produced and used antibiotic worldwide, primarily used in veterinary and human therapies. However, TCs in wastewater have been shown to deteriorate the quality of surface water, groundwater, soil, aquaculture, animals, and humans [2]. Hence, the structure of TCs is similar to naphthalene, which resists degradation and metabolic reactions, thereby explaining the excretion of over 90% of TCs from living organisms via urine and feces, in untransformed form [2-3]. TCs also pose a serious risk to plant metabolism and growth by blocking plant biomass build-up, inhibiting nutrient content, and enhancing both antioxidant enzymes and chemical reactive oxidants [4].

As a result, the occurrence of TCs in water sources poses a significant threat to humans and ecosystems in terms of the development of drug-resistant bacteria and associated toxicity [5]. Doxycycline hyclate (DXC) is a semi-synthetic TC characterized by a broad spectrum of action against Gram-positive and Gram-negative bacteria and is widely used in human and veterinary practice [6]. For all these reasons, it is vital to implement effective, low-cost techniques for treating effluents containing TCs, including DXC. Physical (such as adsorption [7]) and chemical methods have been considered for the remediation of the effluents that contain DXC, such as photolysis, ozonation, H_2O_2 oxidation in the presence of Cu^{2+} as a catalyst, photocatalysis, γ radiolysis, and electron pulse radiolysis of water [8]. A possible alternative to these costly processes could be the Fenton process, which essentially involves the generation of hydroxyl radicals ($\bullet OH$) by dissociating H_2O_2 in an aqueous solution, catalyzed by the Fe^{2+} oxidation to Fe^{3+} . The $\bullet OH$ is

extremely reactive with several organic and inorganic molecules, as they are non-selective. The Fenton process is recognized for its low cost, simplicity, and high rapidity, leading to the formation of non-toxic substances (H_2O and O_2), while the main drawback is the production of $\text{Fe}(\text{OH})_3$ sludge [9-10]. Fenton reaction efficiency is impacted by pH, initial pollutant, oxidant (H_2O_2), and catalyst (Fe^{2+}) amounts. In addition, the excess use of chemicals (Fe^{2+} salt, acid/base H_2O_2) and the cost of H_2O_2 make this method economically disadvantageous [9].

Ultrasound (US) is applied as a new advanced oxidation technology, known as sono-chemical degradation or sonolysis, i.e., degradation induced or enhanced by sonication. This technology treats water contaminated with organic products that conventional techniques cannot treat due to their high chemical stability and low biodegradability [11]. Ultrasonic waves destroy organic materials by producing small bubbles through cavitation in the low-pressure part of the sound. The high-temperature and high-pressure parts are caused by falling and collapsing bubbles, micro-jets, and shock waves. Then, reactive oxygen species such as $\cdot\text{O}$, $\cdot\text{O}^{2-}$, $\cdot\text{OH}$, $\cdot\text{OOH}$, H_2O_2 , etc. [12], are produced by the pyrolysis of water molecules at the point of collapse (hot spots), leading to bond cleavage reactions, in particular of water molecules into $\cdot\text{OH}$ and a hydrogen atom. Thus, US technology plays an important role in the activation and decomposition of oxidants. In addition, organic compounds in the vicinity of a collapsing bubble may undergo degradation by pyrolysis [13]. The $\cdot\text{OH}$ formed causes mineralization of almost all organic molecules.

Sonolysis studies have been carried out with chemical reactants such as Fenton's reagent with three iron forms (Fe^0 , Fe^{2+} , and Fe^{3+}), and these combinations have been shown to improve the degradation of pollutants compared with individually applied processes. With the addition of Fenton's reagent, $\cdot\text{OH}$ can easily be produced so that Fe^{2+} oxidize to Fe^{3+} [11]. Fe^{3+} species then react with H_2O_2 to form Fe-OOH^{2+} complex as an intermediate. When the sonolysis process is applied, a synergistic effect between both processes occurs, spontaneously decomposing Fe-OOH^{2+} by improving the decomposition rate [13]. The Fe^{2+} ions produced further react with H_2O_2 ,

to produce $\cdot\text{OH}$ again, resulting in a cyclic reaction chain. Consequently, the combination of ultrasound and Fenton reagents improves the rate of Fe^{2+} formation in situ and promotes the generation of $\cdot\text{OH}$ [14]. Furthermore, it has been reported that the mineralization of antibiotic molecules is difficult via sonolysis alone, so the combination will also minimize reagent usage and reduce the sludge produced by the Fenton process [12,15]. Therefore, it has been demonstrated that a wide variety of organic pollutants can be degraded by sonication. Thus, sonication is generally considered an environmentally friendly and safe technique for wastewater treatment. However, since sonolysis of organic contaminants has a limited efficiency and consumes considerable amounts of energy, the reduction in energy consumption as well as the improvement in inter-process removal efficiency can be achieved in the case of Sono/Fenton coupling.

A systematic method of process planning, execution, and statistical evaluation is necessary, and only an optimization procedure makes it possible [11-13]. Furthermore, the key to solving any engineering problem lies in improving the performance of a system or process by investigating different parameters in different combinations, to obtain the most effective possible result [16]. Therefore, there are two modes of optimization techniques: one-factor-at-a-time (OFAT) and multivariate methods. These latest approaches have several advantages over OFAT, because they offer an overview of the experimental area studied, investigate the interaction between factors and non-linear relationships with responses, and allow a greater number of results to be obtained with fewer trials [17-18]. Additionally, at each point in the experimental domain, the information is of better quality and can be known through leverage. However, the requirement to minimize the number, expense, duration, and physical energy of experiments originates from experimental design, an alternative and important statistical and mathematical tool for engineering complex and multifactorial problems [19].

Taguchi is a multiparameter optimization statistical method; it is a robust technique that represents the various

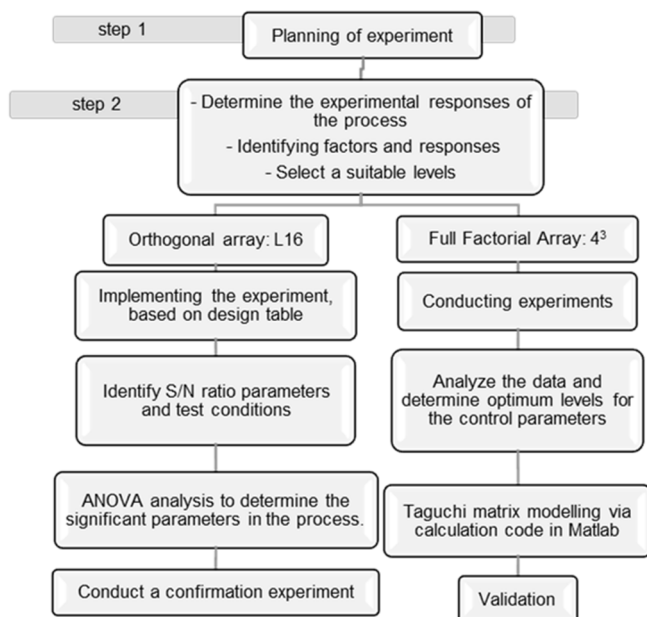


Fig 1. A flowchart of the Taguchi design methodology was utilized for DXC Fenton degradation

combinations of factors. It was applied to find and optimize parameters to achieve the desired response [20]. This technique can be used in two ways: if the output of the orthogonal arrays is optimized with the signal-to-noise ratio (S/N) of the responses instead of the responses themselves, or if the output of the complete array resulting from the factor/level combinations (number of tests equal to the level factor) is then optimized with the answers themselves. This functionality marks the introduction of average factorial effects, interactions, and matrix modeling of the output. The stepwise procedure of the Taguchi method is presented in Fig. 1.

This statistical method has been widely applied to optimize process conditions and formulation in the industry sector. It has also been successfully used in process parameter optimization studies for the removal of organics [19,21-22] and minerals [22-24], from aqueous solutions. However, the literature on the optimization of antibiotic removal from aqueous solutions by AOPs using Taguchi's method is very limited. In this work, three operational parameters were optimized using the Taguchi method to achieve maximum DXC removal from an aqueous solution. There are no reports in the literature on the optimization of commercial-grade DXC degradation using Taguchi experimental designs. In this context, our

study focuses on applying Taguchi's methodology via two experimental designs: orthogonal and full design, to investigate the performance of Taguchi's optimization method.

EXPERIMENTAL SECTION

Materials

DXC (Fig. 2) was provided by Antibiotic-Saidal pharmaceutical group (Medea, Algeria). The chemical structure of DXC is shown in Fig. 2. A hydrogen peroxide (H_2O_2) solution (30%, w/w) and a salt of iron in the form of ferrous sulfate heptahydrate ($\text{FeSO}_4 \cdot 7\text{H}_2\text{O}$) were purchased from Sigma-Aldrich Corporation (St. Louis, MO, USA). All other chemicals were of analytical grade and were used without further purification.

Instrumentation

A measure of DXC concentration was monitored by absorbance using a UV-vis spectrophotometer (Perkin-Elmer Model 550 A). High-performance liquid chromatography (HPLC, Alliance Waters e2695), equipped with a UV-vis detector (Waters 2489) operating at 280 ± 4 nm, an automatic sample injector, a 3D-R solvent delivery system, a thermostatic column compartment set to 45°C , and a reverse-phase column (RP8 with polar embedded groups, $7.5\text{ cm} \times 4.6\text{ mm}$, $3.5\ \mu\text{m}$), was used to acquire the elution data of DXC and its transformation products.

Procedure

Sono-Fenton treatment

US waves were generated using an ultrasonic apparatus with variable power and a constant frequency of 40 kHz (Selecta, France) at room temperature ($25 \pm 1^\circ\text{C}$).

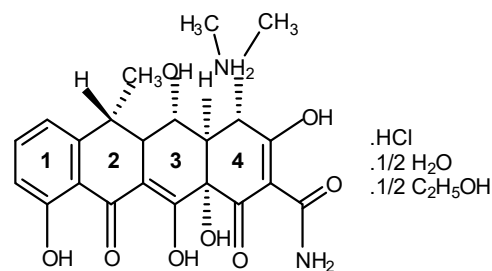


Fig 2. Chemical structure of DXC

Stock solutions of DXC at 1 g/L were used to prepare low-concentration solutions. The reaction mixture was placed in a 1 L Pyrex glass cylinder with a circulating temperature controller. The initial pH of 3 was adjusted by adding H₂SO₄ or NaOH. Chemical reagents such as H₂O₂ and Fe²⁺ were pre-adjusted to the desired concentrations and then added gradually.

Analytical methods

At the completion of the reaction, the reaction mixtures were centrifuged, and the supernatant at the maximum wavelength of DXC (375 nm) was used to estimate the residual DXC concentration after treatment with SF quantitatively [25]. The removal efficiency (RE) was calculated according to Eq. (1);

$$RE(\%) = \frac{C_0 - C_f}{C_0} \times 100\% \quad (1)$$

where C₀ and C_f are the initial and the final DXC concentration (mg L⁻¹). To estimate the DXC transformation, HPLC was used, where the elution was conducted in a gradient program using a binary mobile phase gradient (composed by 2.72 g KH₂PO₄, 0.74 g NaOH, 0.50 g tetrabutylammonium hydrogen sulfate, 0.40 g sodium acetate, and 60 g tertiary butyl alcohol) with a flow rate equal to 0.4 mL min⁻¹. The injection volume was 100 μL, which was conducted with an automatic injector.

Designation, optimization, and modeling of the sono-Fenton combined experiment

The experiment planning is based on the choice of three parameters, namely: the concentration of DXC, H₂O₂, and Fe²⁺, taken at four levels, whose experimental planning methodology was executed according to the steps described in Fig. 1. Therefore, the factors and levels chosen for the present experiment are given in Table 1. The experiments were conducted using a Taguchi design, and the removal efficiency was observed as a response. Finally, each trial's passive response in terms of average removal efficiency at equilibrium was recorded. The

available results from each trial (three results for each) are evaluated in the graphical and statistical analysis tool Minitab® 22 based on mean effects, interactions, S/N ratios, and ANOVA.

Taguchi orthogonal array experiment design. The orthogonal array (OA) experiment is a type of experiment in which the columns for the independent variables are orthogonal to one another. The result can be analyzed using the analysis of variance (ANOVA) and S/N ratio [26]. In Taguchi OA, the S/N ratio is a statistical measure of performance; it represents the deviation of the response from the desired value. The term signal (S) implies the mean value (desirable value), and the noise term (N) shows the standard deviation from the mean (undesirable value). It means that lower variability in the process is ensured by maximizing the S/N ratio. However, depending on the desired response type, Taguchi classified the S/N ratio into three categories: smaller-the-better, larger-the-better, and nominal-the-better. In this study, among the three S/N ratios, the largest one was used to determine optimal combination of parameter levels (Eq. (2)) [20];

$$\frac{S}{N} = -10 \log \left[\frac{1}{n} \sum_{i=1}^n \left(\frac{1}{RE} \right)^2 \right] \quad (2)$$

where RE is the removal efficiency (measured response) and n is the number of repetitions (3) for each test. An L16 OA design was required to study 3 parameters, with 3 different levels for each parameter. In this case, 16 experiments were carried out. Table 2 shows the Taguchi design for the homogeneous sono-Fenton process applied to DXC removal.

Taguchi's Full Array Experiment Design. The full-factorial design (FFD) is the most elementary experimental design. In an FFD, responses are measured for all experimental combinations [21]. Each experimental condition is termed a "run", and the variation of a variable represents each run. Each response

Table 1. Parameters and their levels in the Taguchi design with sono-Fenton process

Independent numerical variables	Symbols	Level 1	Level 2	Level 3	Level 4
Initial DXC concentration (mg L ⁻¹)	X ₁	0.50	2.50	4.50	6.50
Peroxide concentration (mM)	X ₂	0.25	1.25	2.25	3.25
Ferrous concentration (mM)	X ₃	0.05	0.65	1.25	1.85

Table 2. Experiment results (L16) for the SF process of DXC with the OA Taguchi method

Run N ^o	X1	X2	X3	Mean response	Run N ^o	X1	X2	X3	Mean response
1	1	1	1	39.83	9	3	1	3	48.05
2	1	2	2	94.15	10	3	2	4	64.8
3	1	3	3	79.94	11	3	3	1	55.27
4	1	4	4	85.56	12	3	4	2	60.57
5	2	1	2	45.39	13	4	1	4	28.24
6	2	2	1	72.87	14	4	2	3	83.44
7	2	3	4	83.79	15	4	3	2	78.89
8	2	4	3	61.81	16	4	4	1	53.31

is measured for one observation. The set of series constitutes the “design” [19,27]. Considering three parameters with three levels, the experimental stage was constructed on 4^3 (64) trials. These parameters were coded and combined according to a matrix experimental design (Table 1). The output response (y), which expresses RE, is predicted from a matrix model with interactions (Eq. (3)). The FFD methodology consists of evaluating the average effects of the selected parameters and their interactions via the calculated “RE” values obtained after the DXC removal experiments. All the results obtained were used to derive a matrix-type mathematical model (Eq. (6)) for predicting the output response (Y:RE) as a function of the input factors (X_i) and their interaction (X_{ij}). All the steps involved in developing the model were carried out using a MATLAB calculation code;

$$y(i, j, k) = M + EX1_i + EX2_j + EX3_k + INX1_i X2_j + INX1_i X3_k + INX2_j X3_k \quad (3)$$

where y is the response and i , j , and k are the levels of the factors $X1$, $X2$, and $X3$, respectively.

Phytotoxicity tests

Phytotoxicity tests were conducted to assess the effect of DXC and its transformation products obtained after SFO on vegetation. Experiments were conducted to find out the toxicity of liquid samples on seed germination and root elongation to explore the possible reuse of treated samples in irrigation fields [25]. The original DXC solution and the residues extracted from ethyl acetate were dried and dissolved separately in sterile distilled water to prepare a solution with a final concentration of 100 ppm. The experiments were carried out (at room

temperature) on two types of seed commonly used in Algerian agriculture: *Sorghum vulgare* and *Pisum sativum* L. Ten seeds of each plant were sown in 20 g of sand previously washed and placed in a plastic pot. The phytotoxicity study was carried out by spraying the seeds of each plant with 5 mL of distilled water as a control, the initial DXC solution, and the extracted solution per day. Germination, plumule (shoot) and radicle (root) length were recorded after 7 d [25]. Relative seed germination (SG), relative root growth (RRG), and germination index (GI) were calculated using Eq. (4–6) [28].

$$SG(\%) = \frac{\text{Number of germinated seeds in assay}}{\text{Number of germinated seeds in control}} \times 100\% \quad (4)$$

$$RRG(\%) = \frac{\text{Mean root length in assay}}{\text{Mean root length in control}} \times 100\% \quad (5)$$

$$GI(\%) = \frac{SG(\%) \times RRG(\%)}{100} \quad (6)$$

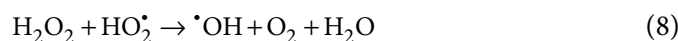
RESULTS AND DISCUSSION

Taguchi Array Design: Optimization and Modeling

Taguchi OA experimental design

To optimize 3 experimental variables of DXC elimination, corresponding to the factors $X1$, $X2$, and $X3$, which were studied at four levels using an OA design, a total of 16 experiments (L16 design, Table 2) were conducted. A range of 0 to 95% values was obtained for removal efficiency. According to the mean values of the results, combinations 13 and 2 showed the lowest and highest elimination efficiencies, respectively. The main effect plots were determined through the S/N ratio, expressed in terms of dispersion around a target value. The S/N ratio measures the level of performance and the

effects of noise factors on it. For the present study, the results of the responses to each experimental factor at its respective level were analyzed by calculating the average S/N ratio at each level for each factor. Fig. 3 shows a more significant influence of H₂O₂ concentration, followed by DXC, and a near effect of Fe²⁺ dose. Considering the response of the S/N ratio to H₂O₂ dose (factor X2), the average S/N ratio increases up to a H₂O₂ concentration of 2.5 mM (level 2). This phenomenon can be attributed to the formation of excess $\cdot\text{OH}$ radicals [22]. A further increase in the concentration of H₂O₂ in the reaction medium leads to a reduction in removal efficiency between concentrations of 2.5 and 3.5 mM (levels 3 and 4). In fact, H₂O₂ acts as a $\cdot\text{OH}$ radical scavenger at high concentrations and affects the concentration of $\cdot\text{OH}$. This is because, on the one hand, $\cdot\text{OH}$ can react with H₂O₂ to generate hydroperoxyl radicals (HO₂ \cdot) (Eq. (7)), which have a lower reaction rate and oxidation power than $\cdot\text{OH}$, and do not participate in the oxidative degradation of organic compounds [13,20]. On the other hand, $\cdot\text{OH}$ can also react with another $\cdot\text{OH}$ to produce H₂O₂, or respond with the HO₂ \cdot to generate $\cdot\text{OH}$ shown in Eq. (8) and (9) [20].



Similarly, the second most important controllable factor is the concentration of pollutants, which is one of

the most important factors in Fenton's processes. Fig. 3 clearly shows that increasing the DXC concentration from 0.5 to 4.5 mg L⁻¹ reduces the S/N ratio to a given level. It is assumed that, by increasing the number of pollutant molecules in the reaction mixture, the competitive use of $\cdot\text{OH}$ increases with the intermediate products, leading to a decrease in removal efficiency. Malakootian et al. [13] studied the transformation of TC, which differs from DXC only in the position of the OH at ring 3 instead of ring 2, using the US-Fenton and reported that the rate of decomposition depends on the initial concentration of TC; consequently, the rate of decomposition decreases significantly with an increase in the initial concentration of TC. For the factor Fe²⁺ dose, the average difference between the S/N ratios at the highest and lowest levels is not so significant concerning H₂O₂ concentration (a value of 1.89 vs. 5.1 for H₂O₂). According to Fig. 3 the S/N ratio improved with increasing Fe²⁺ dosage from 0.05 to 0.65 mM, then reduced above this dose. So, the presence of an iron ion source in sono-catalytic processes provides additional nuclei and levels for cavitation, which will increase the number of bubbles and radicals. In other terms, Fe²⁺ cause an increase in the decomposition of H₂O₂ produced during the cavitation process, leading to an increase in the free radicals produced in aqueous environments (Eq. (10–12)). The results of a study by Malakootian et al. [13] and Wang et al. [29] using the sono-Fenton-like process and the

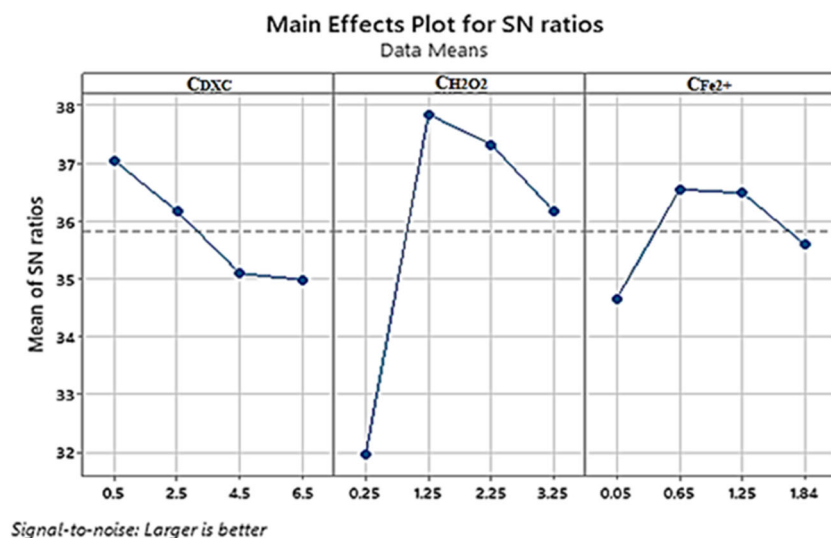
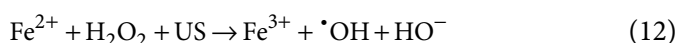
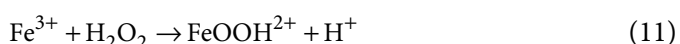
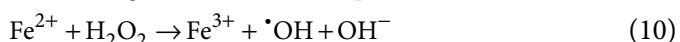


Fig 3. Effect of process parameters on S/N ratio

sono-Fenton process for the decomposition of the TC showed that the removal efficiency was increased by increasing the Fe^{2+} level. However, after this increase, the efficiency decreased. Many researchers have pointed out that the use of a higher Fe^{2+} concentration could lead to self-evacuation of the $\cdot\text{OH}$ by converting it to hydroxyl ions during Fe^{2+} oxidation (Eq. (13)) [30-31].



The main effect represents the average effect of an independent variable on a dependent variable, averaged over the levels of all the independent variables. Analyzing the main effects of the parameters (Fig. 4), the general patterns of factor influence on the process can be determined. These are similar to those of the S/N ratios, where the results show that H_2O_2 is a significant parameter to enhance DXC removal up to a critical concentration, as is the case with Fe^{2+} , while DXC negatively impacts the removal efficiency.

In Taguchi design experiments, ANOVA is generally

performed to evaluate the effect of parameters on the mean response and the S/N ratio. Analysis of variance ANOVA is a robust method used to determine the relative relevance of each parameter using statistical data, such as sequential (Seq) and adjusted (Adj) sum of squares (SS), mean square (MS), F-value (F), P-value (P), and contribution (%). The parameter with the highest sum of squares has the greatest influence on the experimental parameters [19,32]. Thus, the F-test is a tool for checking which process parameters have a significant effect on removal efficiency. A P value of less than 0.05 indicates that the parameter is significant [17].

As shown in Table 3, the ANOVA results clearly indicate that H_2O_2 concentration exerts the most statistically significant influence on the degradation efficiency, with a P-value of 0.004 ($P < 0.05$), confirming its effect is significant at the 95% confidence level. The F-statistic of 7.82, corresponding to a relatively high mean square (MS) value of 1182.2, further supports the conclusion that variation in H_2O_2 concentration introduces substantial variance in the response variable. Its Seq SS (3547.0) and dominant percentage contribution (74.54%) suggest that this factor explains

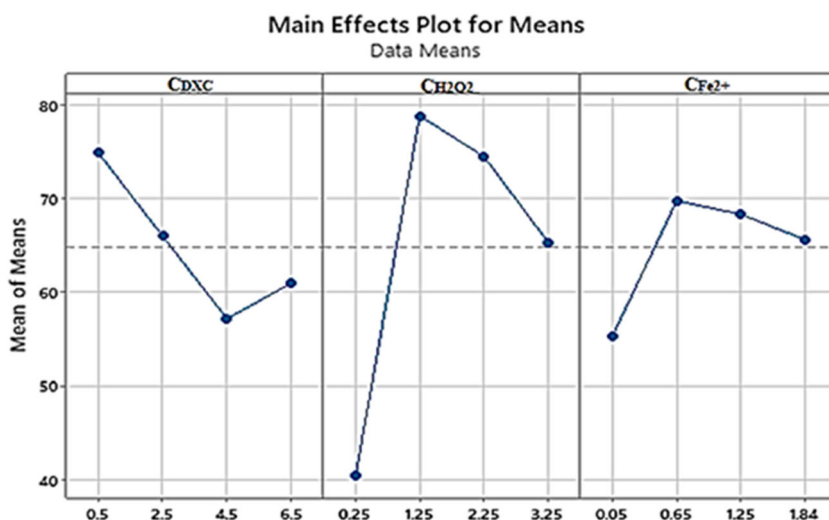


Fig 4. Effect of process parameters on removal efficiency

Table 3. ANOVA results for DXC removal

Factor	d.f	Seq SS	Adj SS	Adj MS	F	P	Contribution (%)
C_{DXC} (mg L^{-1})	3	702.40	702.40	234.10	0.60	0.625	14.76
$C_{\text{H}_2\text{O}_2}$ (mM)	3	3547.00	3547.00	1182.20	7.82	0.004	74.54
$C_{\text{Fe}^{2+}}$ (mM)	3	509.30	509.30	169.80	0.42	0.742	10.70

the majority of the total variance observed in the system. From a mechanistic standpoint, this aligns with the central role of H_2O_2 in Fenton-based advanced oxidation processes, where it acts as the primary source of $\cdot\text{OH}$ in the presence of Fe^{2+} catalysts. The generation of $\cdot\text{OH}$ is a key rate-determining step in the degradation of recalcitrant pollutants like DXC. As such, increasing H_2O_2 concentration enhances the oxidative capacity of the system, resulting in higher degradation rates, which is reflected quantitatively in the model.

In contrast, both initial DXC and Fe^{2+} concentration showed statistically non-significant effects with P-values of 0.625 and 0.742, respectively. Their low F-values (0.60 for DXC and 0.42 for Fe^{2+}) and limited percentage contributions (14.76 and 10.70%) suggest that, within the tested experimental domain, changes in these parameters do not produce substantial variation in removal efficiency. At higher DXC concentrations, the number of pollutant molecules may exceed the reactive species available, resulting in a plateau in the degradation rate. Similarly, excess Fe^{2+} can result in the scavenging of hydroxyl radicals via side reactions (Eq. (13)), thereby reducing the overall process efficiency. The relatively low Adj SS values for these two factors imply limited explanatory power regarding response variability, supporting the prioritization of H_2O_2 level for process optimization. These results underline the importance of balancing reagent concentrations to maximize radical generation while minimizing inhibitory or competing reactions in Fenton-like systems. Fig. 5 shows the relative contributions of the three parameters studied to RE of DXC. The H_2O_2 dose parameter has 74.53%, while the DXC concentration and Fe^{2+} parameters have the lowest contributions, at 14.76 and 10.7%, respectively, to transformation efficiency. In their study of Congo red degradation by the US-assisted Fenton process, Nawaz et al. [33] observed that the addition of H_2O_2 significantly increased degradation efficiency. This behavior may be attributed to the limited oxidation capacity at low H_2O_2 concentrations compared to $\cdot\text{OH}$. In other words, at low concentrations, H_2O_2 cannot generate sufficient $\cdot\text{OH}$ and the oxidation rate is slow.

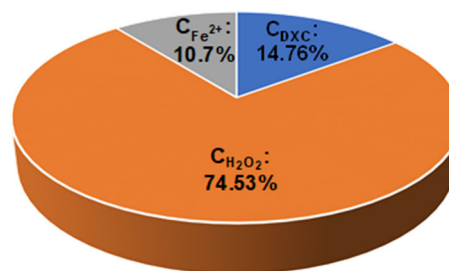


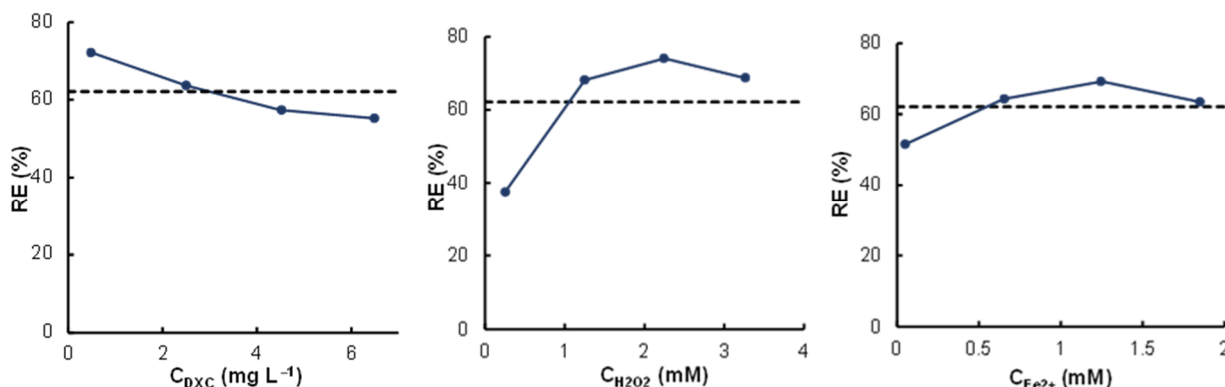
Fig 5. Contribution of parameters

Full factorial design (FFD)

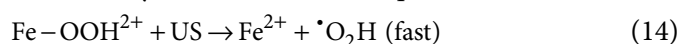
The FFD needs more experimental points, as it provides more information on the effect of different combinations. The results of the various combinations of factors: concentrations of DXC (C_{DXC} , 0.5–6.5 mg L^{-1}), H_2O_2 ($C_{\text{H}_2\text{O}_2}$, 0.25–3.25 mM), and Fe^{2+} ($C_{\text{Fe}^{2+}}$, 0.05–1.85 mM) are detailed in Table 4. The optimum conditions for high DXC removal efficiency, measuring 94.15%, corresponding to test No. 6, in combination: 122, with concentrations of 0.5 mg L^{-1} of DXC, 1.25 mM of H_2O_2 and 0.65 mM of Fe^{2+} , were therefore considered the optimum levels. Indeed, the results of the average effects are plotted to show the influence of the independent parameters studied on the sono-Fenton oxidation of DXC, as well as the parameter with the greatest impact on the Fenton treatment (Fig. 6). For the concentration ranges considered in the DXC study, it was found that: for the effect of DXC concentration, as the DXC content in the reaction medium increases, its transformation is reduced, which may be due to the excess of DXC molecules over the number of $\cdot\text{OH}$ present in the reaction medium. A significant improvement in DXC removal is achieved for H_2O_2 concentrations ranging from 0.25 to 2.25 mM. A reduction was observed at a concentration of 3.25 mM, which is due to the scavenging of $\cdot\text{OH}$ by H_2O_2 molecules (Eq. (14)). As a result, a concentration of 2.25 mM is considered to be optimal. Regarding Fe^{2+} , given that these cations are indispensable in the initiation reaction of the radical process of $\cdot\text{OH}$ generation, their content has a considerable influence from an efficiency point of view, reflected by a significant increase in the RE up to a concentration of 1.25 mM (level 3). An inhibition of the transformation of DXC is reached. This influence is attributed to Fe^{2+}

Table 4. Experiment results for the sono-Fenton process of DXC removal using full factorial design

Run N°	RE (%)	Run N°	RE (%)	Run N°	RE (%)	Run N°	RE (%)	Run N°	RE (%)
1	39.83	14	90.39	27	84.03	40	64.80	53	24.64
2	41.20	15	92.50	28	83.79	41	85.27	54	70.43
3	84.56	16	85.56	29	53.32	42	83.55	55	43.44
4	35.22	17	17.55	30	58.13	43	85.84	56	61.86
5	92.33	18	18.39	31	61.81	44	89.25	57	59.24
6	94.15	19	76.79	32	75.75	45	71.90	58	78.89
7	91.57	20	30.46	33	16.66	46	60.57	59	77.40
8	86.01	21	32.87	34	22.14	47	66.49	60	81.88
9	89.30	22	66.25	35	56.05	48	73.35	61	73.31
10	90.46	23	64.64	36	32.01	49	10.5	62	51.03
11	79.94	24	38.67	37	73.22	50	17.25	63	31.52
12	84.25	25	82.00	38	47.98	51	15.33	64	75.32
13	88.27	26	83.05	39	68.32	52	14.24	Mean (%)	62.13

**Fig 6.** Effect of process parameters on RE of DXC in sono-Fenton process (pH = 3)

oxidation by $\cdot\text{OH}$, as shown in Eq. (13).



A study of potential interactions was conducted using interaction diagrams. Each diagram depicts the interaction between two factors. Fig. 7 displays matrix plots for the three studied factors. These graphs depict a complete matrix of interactions. Fig. 7(a) shows the interaction diagrams for DXC and H_2O_2 concentrations taken at different levels. The interactions between X1 (1×4) and X2 (2×4) are significant among the factors. Fig. 7(b) reveals that the interaction between DXC concentration (X1) and Fe^{2+} dose (X3) is significant between X1 (2×4) and X3 (2×4). The remaining interaction presented in Fig. 7(c), shows that X2 (1×3) and X3 (1×4) have an almost rectilinear effect, forming a parallel line, meaning these two conditions are not linked.

On the other hand, the interaction between X2 (3) and X3 (2×4) showed a more significant relationship.

These considerations were referred to the reports of Morshed et al. [19], who noted that interaction between factors exists if non-parallel lines represent the relationship, while parallel lines indicate that there is no relationship between the parameters. The general scenario shows that removal efficiency increases with increasing H_2O_2 and Fe^{2+} level up to a given value and that, at the same time, the DXC concentration decrease RE, which is compatible with the main effects. This also indicates that interaction diagrams are suitable for exploring process parameters. To evaluate the elimination efficiency at the levels studied and at other levels, a MATLAB 7 software run was performed after the program was developed. The Taguchi matrix model,

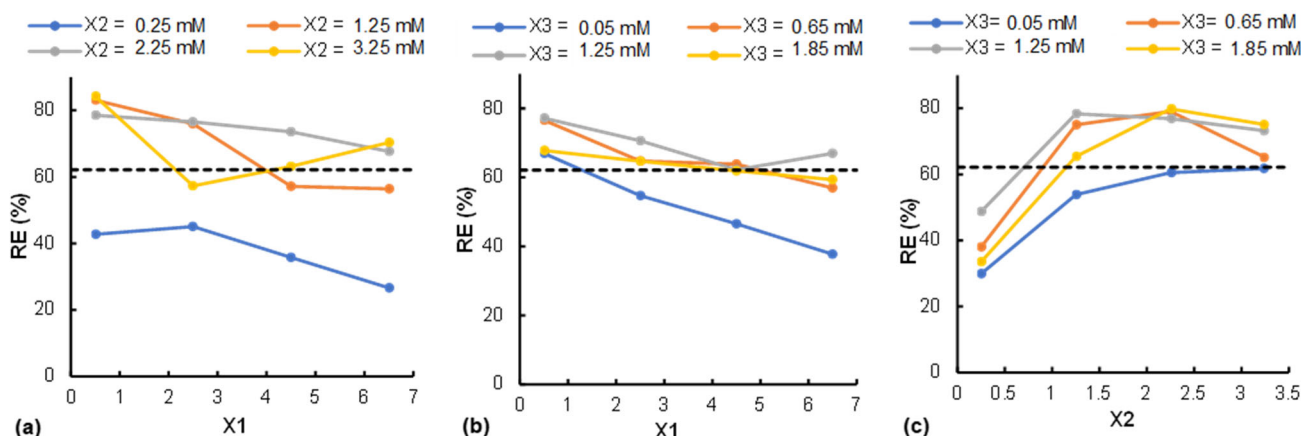


Fig 7. Interactions between: (a) C_{DXC} and $C_{H_2O_2}$, (b) C_{DXC} and $C_{Fe^{2+}}$, and (c) $C_{H_2O_2}$ and $C_{Fe^{2+}}$ in the SF process

expressed by Eq. (15), allows the output (RE) to be predicted as a function of the input factors and their interaction.

$$\begin{aligned}
 RE(i,j,k) = & 62.13 + (10.0225 \ 1.5825 \ -4.7362 \ -6.8688)(C_{DXC}) \\
 & + (-24.5625 \ 6.0000 \ 11.9350 \ 6.6275)(C_{H_2O_2}) \\
 & + (-106231 \ 2.1675 \ 7.1281 \ 1.3275)(C_{Fe^{2+}}) \\
 & + (INC_{DXC})^t \begin{pmatrix} -4.8312 & 4.9188 & -5.5437 & 5.4562 \\ 5.9538 & 6.2013 & 0.8763 & -13.0313 \\ 2.9400 & -6.2575 & 4.2050 & -0.8875 \\ -4.0625 & -4.8625 & 0.4625 & 8.4625 \end{pmatrix} (INC_{H_2O_2}) \\
 & + (INC_{DXC})^t \begin{pmatrix} 5.4594 & 202863 & -2.0819 & -5.6637 \\ 1.6519 & -1.1187 & -0.2169 & -0.3162 \\ -0.2019 & -0.6950 & -2.2906 & 3.1875 \\ -6.9094 & -0.4725 & 4.5894 & 2.7925 \end{pmatrix} (INC_{Fe^{2+}}) \\
 & + (INC_{H_2O_2})^t \begin{pmatrix} 2.9969 & -1.6837 & 4.0431 & -5.3562 \\ -3.6856 & 4.7113 & 3.0406 & -4.0662 \\ -2.9331 & 2.8113 & -4.3344 & 4.4563 \\ 3.6219 & -5.8387 & -2.7494 & 4.9663 \end{pmatrix} (INC_{Fe^{2+}})
 \end{aligned} \quad (15)$$

where: IN: factor interaction, and IN^t: transpose factor interaction

Fig. 8 compares experimental and predicted values for DXC removal efficiency from aqueous solution. As this figure illustrates, the predicted responses were in good agreement with the measured ones. In Fig. 8(a), the points in a circle are the residuals. If these points are close to the bisector, they indicate the normality of the residuals. As this figure shows, this is confirmed, hence the normality of the residuals. To assess the model's adequacy, the mathematical model's assumptions were examined using the diagnostic method. In Fig. 8(a), the points in a circle are the residuals. If these points are close

to the bisector, they indicate the normality of the residuals. In Fig. 8(b), the residual curves of the established model are distributed randomly and without any particular process, and due to the absence of any trend, it can be confirmed that this model is appropriate and that, consequently, the assumption of normality of the residuals is acceptable and can be used to predict the responses of DXC elimination efficiency [16].

DXC Sono-Fenton Degradation Pathway

In a previous study, the characterization of degradation products detected via the photo-Fenton process was carried out, where it was found that the spectra were almost similar in pattern [34]. The DXC spectrum shown in Fig. 9 displays 3 absorption bands characteristic of the aromatic ring, 2 in the UV-B range at 245 and 275 nm (ring 4), and the third in the UV-A region at 375 nm, which corresponds to the phenolic diketone of the DXC (rings 1-2-3) [30].

After treatment of the DXC solution (at 0.5 mg/L) under optimum conditions, UV-vis spectral and HPLC analysis of the solution treated by the sono-Fenton process (Fig. 9(a) and (b)), show the disappearance of all three absorption bands and the formation of a very weak absorption band between 200 and 210 nm. Several reaction pathways have been proposed for the transformation reactions of the DXC molecule through the attack of radicals, generated via POAs, such as photo-Fenton [34], Fenton [8], sonolysis [14], photolysis, peroxidation, photoperoxidation, ozonation, homogeneous [35] and heterogeneous photocatalytic

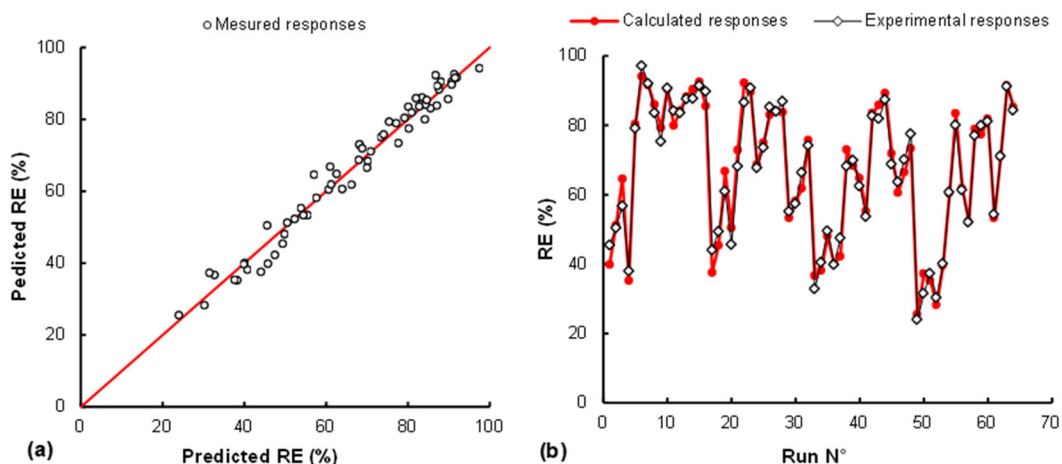


Fig 8. The experimental RE plotted against the predicted values calculated from the FFD model – (a) Taguchi model and (b) diagnostics plots for DXC removal

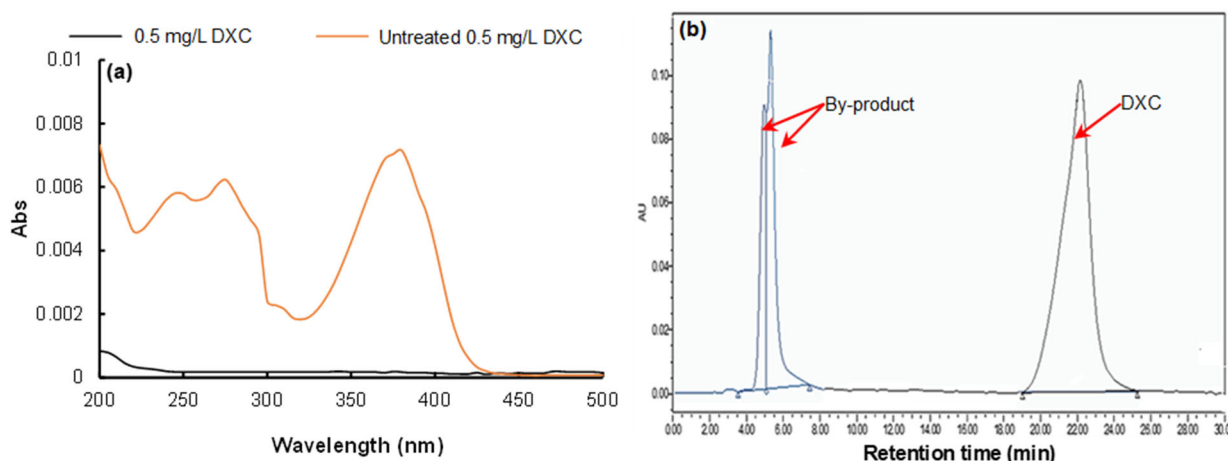


Fig 9. (a) UV-vis spectra of DXC before and after sono-Fenton treatment and (b) HPLC chromatograms of DXC aqueous solution before and after SF treatment

processes [36-37], these studies showed an oxidation with the formation of intermediates of smaller size. Thus, it has been reported that $\cdot\text{OH}$ radicals involve a non-selective attack concerning the cleavage of functional groups through dehydroxylation, deamination, oxidation and aromatic ring cleavage reactions [38].

The difference in by-products between POAs could be due to the difference in the amount of $\cdot\text{OH}$ radicals produced, the nature of other generated radicals, which are less selective (superoxide anions, singlet oxygen, hydroperoxyl, etc.) than $\cdot\text{OH}$, hydroxylation of DXC aromatic rings, and energy input. So far, no literature has been found to correlate the BP formed and their degradation mechanism, particularly for low-mass BP

[39]. Table 5 summarizes previous results on the elimination of DXC using the laboratory-scale Fenton processes.

In the literature, there have been no previous reports on the comparison of DXC degradation by sonification processes. Sonification has been applied individually to remove pharmaceutical pollutants from the TC family, or in combination with the Fenton process, ozone, Fe_3O_4 magnetic nanoparticles, or titanium dioxide (TiO_2). All these works report that the RE does not reach 90% with US alone, but it improves significantly in the presence of a catalyst or an oxidizing agent. However, regarding the application of the Fenton process alone, the RE of TC molecules is also too low compared to its coupling in

Table 5. Comparison of DCX removal efficiency with previous work on TCs using Fenton processes

TC pollutant	C_{TCs} (mg L ⁻¹)	RE (%)	Fenton process	Reference
DXC	10.25	53.00	Fenton	[37]
DXC	2.50	79.00	Photo-Fenton	[34]
DXC	17.67	95.07	Photo-Fenton	[30]
DXC	0.50	99.60	UV/H ₂ O ₂	[35]
			O ₃	
DXC	0.50	26.40	Photolysis	[35]
DXC	0.50	5.00	Peroxidation	[35]
DXC	10.25	35.00	Fenton-based process (H ₂ O ₂ /Fe(III))	[37]
DXC	10.25	100.00	UV/H ₂ O ₂ /Fe(III)	[37]
DXC	2.00	66.00	Ultrasonification	[14]
TC	20.00	88.36	Ultrasonification	[13]
CTC	5.10	67.00	Ultrasonification	[39]
CTC	5.10	76.00	Fenton	[39]
CTC	5.10	82.00	Ferro-sonification	[39]
DXC	0.50	94.15	Ultrasound/Fenton	This study

CTC: Chlortetracycline

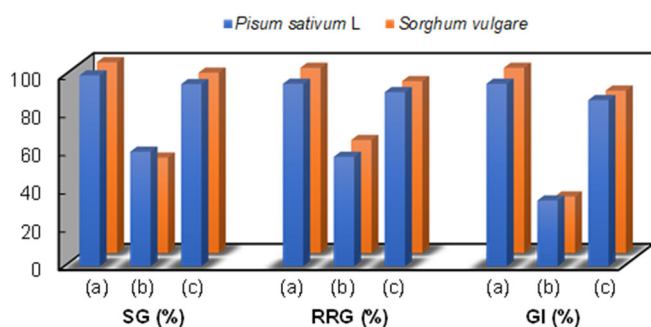


Fig 10. Phytotoxicity results of plants irrigated with the DXC and its metabolites solutions, (a) control; (b) plant irrigated with the raw DXC solution (100 ppm); (c) plant irrigated with the extract solution (100 ppm)

homogeneous or heterogeneous media, where RE exceeding 90% have been achieved. For the present work, these observations are confirmed by RE of more than 94% in the presence of Fenton reagents coupled with US.

Phytotoxicity Test

The various germination parameters obtained and presented in Fig. 10 have clearly demonstrated a tendency towards reduced phytotoxicity after DXC treatment. Root elongation and seed germination of *Lepidium sativum* L. and *Sorghum vulgare* were severely retarded (GI of 34.392 and 29.61%, respectively), indicating that DXC has a

noticeable toxicity. For extracts obtained after SF treatment, GI increased to 87.04 and 85.15%. Based on GI percentages, compounds (and by-products) can be classified into three categories: high phytotoxicity (GI > 80%), low phytotoxicity (GI < 50%), and moderate phytotoxicity (50% < GI < 80%). It is interesting to note that the treatment was effective and that DOX by-products are not phytotoxic, and their transformation products are not phytotoxic to the seeds tested.

CONCLUSION

This study is the first attempt to systematically process-optimize DXC solutions by the sono-Fenton method using two experimental designs: orthogonal arrays design (OA: L16) and full factorial design (FFD: L64). The interesting results obtained in the context of this research suggest that the Taguchi approach, although simple, is useful in the systematic study of the sono-Fenton process and enables more information to be obtained in less time and with fewer resources than full factorial designs. On the other hand, the FFD approach enabled the entire range of parameters influencing the process and their interactions to be studied, while establishing a powerful matrix model. In other words, the highest efficiency of DXC removal using FFD and

OA was the same and was 94.15%. The ANOVA analysis of the two Taguchi approaches both indicated that the three factors studied presented different effects on the oxidation of DXC, where H₂O₂ had the greatest impact compared to DXC and Fe²⁺. Characterization of the degradation by-products of the DXC molecule showed that this molecule is transformed by the •OH generated during the sequential reactions of the sono-Fenton process. Consequently, because of the large and already existing quantities of antibiotics being present in aqueous wastewater solutions, this method may well be adopted as a cost-effective way of purifying environments polluted by pharmaceuticals.

■ ACKNOWLEDGMENTS

The authors are grateful to the Laboratory of BioMaterial and Transport Phenomena (LBMTTP) for help and encouragement. The authors also thank Pr. Bouaziz M.N., University of MEDEA, for its immense contribution.

■ CONFLICT OF INTEREST

All authors declare no conflicts of interest.

■ AUTHOR CONTRIBUTIONS

Nabila Boucherit: writing – original draft, writing – review and editing, conceptualization, methodology, supervision, resources. Mohamed Barki: conceptualization, visualization. Achouak Madani: conceptualization, writing – review. Abdelkarim Brahimi: writing – review, methodology, supervision, resources. Nassiba Mimi: writing – review, methodology, supervision, resources.

■ REFERENCES

- [1] Grenni, P., Ancona, V., and Barra Caracciolo, A., 2018, Ecological effects of antibiotics on natural ecosystems: A review, *Microchem. J.*, 136, 25–39.
- [2] Xu, L., Zhang, H., Xiong, P., Zhu, Q., Liao, C., and Jiang, G., 2021, Occurrence, fate, and risk assessment of typical tetracycline antibiotics in the aquatic environment: A review, *Sci. Total Environ.*, 753, 141975.
- [3] Antón-Herrero, R., García-Delgado, C., Alonso-Izquierdo, M., García-Rodríguez, G., Cuevas, J., and Eymar, E., 2018, Comparative adsorption of tetracyclines on biochars and stevensite: Looking for the most effective adsorbent, *Appl. Clay Sci.*, 160, 162–172.
- [4] Han, T., Liang, Y., Wu, Z., Zhang, L., Liu, Z., Li, Q., Chen, X., Guo, W., Jiang, L., Pan, F., Ge, S., Mi, Z., Liu, Z., Huang, H., Li, X., Zhou, J., Li, Y., Wang, J., Zhang, Z., Tang, Y., Yang, L., and Wu, M., 2019, Effects of tetracycline on growth, oxidative stress response, and metabolite pattern of ryegrass, *J. Hazard. Mater.*, 380, 120885.
- [5] Warner, A.J., Hathaway-Schrader, J.D., Lubker, R., Davies, C., and Novince, C.M., 2022, Tetracyclines and bone: Unclear actions with potentially lasting effects, *Bone*, 159, 116377.
- [6] Graber, E.M., 2021, Treating acne with the tetracycline class of antibiotics: A review, *Dermatol. Rev.*, 2 (6), 321–330.
- [7] Aniagor, C.O., Igwegbe, C.A., Ighalo, J.O., and Oba, S.N., 2021, Adsorption of doxycycline from aqueous media: A review, *J. Mol. Liq.*, 334, 116124.
- [8] Borghi, A.A., Silva, M.F., Al Arni, S., Converti, A., and Palma, M.S.A., 2015, Doxycycline degradation by the oxidative Fenton process, *J. Chem.*, 2015 (1), 492030.
- [9] Jiang, Y., Ran, J., Mao, K., Yang, X., Zhong, L., Yang, C., Feng, X., and Zhang, H., 2022, Recent progress in Fenton/Fenton-like reactions for the removal of antibiotics in aqueous environments, *Ecotoxicol. Environ. Saf.*, 236, 113464.
- [10] Baran, W., and Adamek, E., 2023, Degradation of veterinary antibiotics by Fenton process: Products identification and toxicity assessment, *Chemosphere*, 341, 139854.
- [11] Moradi, M., Elahinia, A., Vasseghian, Y., Dragoi, E.N., Omidi, F., and Mousavi Khaneghah, A., 2020, A review on pollutants removal by sono-photo-Fenton processes, *J. Environ. Chem. Eng.*, 8 (5), 104330.
- [12] Liu, P., Wu, Z., Abramova, A.V., and Cravotto, G., 2021, Sonochemical processes for the degradation of antibiotics in aqueous solutions: A review, *Ultrason. Sonochem.*, 74, 105566.

- [13] Malakootian, M., and Asadzadeh, S.N., 2020, Oxidative removal of tetracycline by sono Fenton-like oxidation process in aqueous media, *Desalin. Water Treat.*, 193, 392–401.
- [14] Cárdenas Sierra, R.S., Zúñiga-Benítez, H., and Peñuela, G.A., 2021, Elimination of cephalixin and doxycycline under low frequency ultrasound, *Ultrason. Sonochem.*, 79, 105777.
- [15] Wang, C., and Huang, B.M., 2017, Degradation of tetracycline by advanced oxidation processes: Sono-Fenton and ozonation processes, *Desalin. Water Treat.*, 96, 161–168.
- [16] Yousefi, Z., Zafarzadeh, A., and Ghezeli, A., 2018, Application of Taguchi's experimental design method for optimization of Acid Red 18 removal by electrochemical oxidation process, *Environ. Health Eng. Manage. J.*, 5, 241–248.
- [17] Nandhini, M., Suchithra, B., Saravanathamizhan, R., and Prakash, D.G., 2014, Optimization of parameters for dye removal by electro-oxidation using Taguchi design, *J. Electrochem. Sci. Eng.*, 4 (4), 227–234.
- [18] Paliy, O., and Shankar, V., 2016, Application of multivariate statistical techniques in microbial ecology, *Mol. Ecol.*, 25 (5), 1032–1057.
- [19] Morshed, M.N., Pervez, M.N., Behary, N., Bouazizi, N., Guan, J., and Nierstrasz, V.A., 2020, Statistical modeling and optimization of heterogeneous Fenton-like removal of organic pollutant using fibrous catalysts: A full factorial design, *Sci. Rep.*, 10 (1), 16133.
- [20] Sohrabi, M.R., Khavaran, A., Shariati, S., and Shariati, S., 2017, Removal of Carmoisine edible dye by Fenton and photo Fenton processes using Taguchi orthogonal array design, *Arabian J. Chem.*, 10, S3523–S3531.
- [21] Barragán-Trinidad, M., Guadarrama-Pérez, O., Guillén-Garcés, R.A., Bustos-Terrones, V., Trevino-Quintanilla, L.G., and Moeller-Chávez, G., 2023, The Grey-Taguchi method, a statistical tool to optimize the photo-Fenton process: A review, *Water*, 15 (15), 2685.
- [22] Adar, E., 2020, Optimization of triple dye mixture removal by oxidation with Fenton, *Int. J. Environ. Sci. Technol.*, 17 (11), 4431–4440.
- [23] Fernández-López, J.A., Angosto, J.M., Roca, M.J., and Doval Miñarro, M., 2019, Taguchi design-based enhancement of heavy metals bioremoval by agroindustrial waste biomass from artichoke, *Sci. Total Environ.*, 653, 55–63.
- [24] Aziri, S., and Meziane, S., 2017, Optimization of process parameters for Cr(VI) removal by seed powder of prickly pear (*Opuntia ficus-indica* L.) fruits using Taguchi method, *Desalin. Water Treat.*, 81, 118–122.
- [25] Boucherit, N., Abouseoud, M., and Adour, L., 2018, Direct yellow degradation by combined Fenton-enzymatic process, *Nova Biotechnol. Chim.*, 17 (2), 160–171.
- [26] Hsieh, L.L., Kang, H.J., Shyu, H.L., and Chang, C.Y., 2009, Optimal degradation of dye wastewater by ultrasound/Fenton method in the presence of nanoscale iron, *Water Sci. Technol.*, 60 (5), 1295–1301.
- [27] Salea, R., Widjojokusumo, E., Hartanti, A.W., Veriansyah, B., and Tjandrawinata, R.R., 2013, Supercritical fluid carbon dioxide extraction of *Nigella sativa* (black cumin) seeds using Taguchi method and full factorial design, *Biochem. Compd.*, 1, 1.
- [28] Ravindran, B., Kumari, S.K.S., Stenstrom, T.A., and Bux, F., 2016, Evaluation of phytotoxicity effect on selected crops using treated and untreated wastewater from different configurative domestic wastewater plants, *Environ. Technol.*, 37 (14), 1782–1789.
- [29] Wang, C., and Jian, J.J., 2015, Degradation and detoxicity of tetracycline by an enhanced sonolysis, *J. Water Environ. Nanotechnol.*, 13 (4), 325–334.
- [30] Bensaibi, F., Chabani, M., Bouafia, S., and Djelal, H., 2023, Doxycycline removal by solar photo-fenton on a pilot-scale composite parabolic collector (CPC) reactor, *Processes*, 11 (8), 2363.
- [31] Yildiz, S., Mihçioğur, H., and Olabi, A., 2023, Experimental study of oxytetracycline degradation using Fenton-like processes, *Int. J. Environ. Sci. Technol.*, 20 (10), 11049–11060.
- [32] Sruthi, P.S., and Shanmugasundaram, S., 2022, Optimization of process parameters by Taguchi method for the development of biosensor for the

- detection of acrylamide in fried foods, *Pharma Innovation*, 11 (10S), 4–10.
- [33] Nawaz, S., Siddique, M., Khan, R., Riaz, N., Waheed, U., Shahzadi, I., and Ali, A., 2022, Ultrasound-assisted hydrogen peroxide and iron sulfate mediated Fenton process as an efficient advanced oxidation process for the removal of Congo red dye, *Pol. J. Environ. Stud.*, 31 (3), 2749–2761.
- [34] Boucherit, N., Hanini, S., Ibrir, A., Laidi, M., and Fissa, M., 2024, Prediction of doxycycline removal by photo-Fenton process using an artificial neural network - multilayer perceptron model, *Chem. Ind. Chem. Eng. Q.*, 31 (1), 13–21.
- [35] Spina-Cruz, M., Maniero, M.G., and Guimarães, J.R., 2019, Advanced oxidation processes on doxycycline degradation: Monitoring of antimicrobial activity and toxicity, *Environ. Sci. Pollut. Res.*, 26 (27), 27604–27619.
- [36] Hong, P., Li, Y., He, J., Saeed, A., Zhang, K., Wang, C., Kong, L., and Liu, J., 2020, Rapid degradation of aqueous doxycycline by surface $\text{CoFe}_2\text{O}_4/\text{H}_2\text{O}_2$ system: Behaviors, mechanisms, pathways and DFT calculation, *Appl. Surf. Sci.*, 526, 146557.
- [37] Bolobajev, J., Trapido, M., and Goi, A., 2016, Effect of iron ion on doxycycline photocatalytic and Fenton-based autocatalytic decomposition, *Chemosphere*, 153, 220–226.
- [38] Berdini, F., Otalvaro, J.O., Avena, M., and Brigante, M., 2022, Photodegradation of doxycycline in water induced by TiO_2 -MCM-41. Kinetics, TOC evolution and reusability, *Results Eng.*, 16, 100765.
- [39] Pulicharla, R., Brar, S.K., Rouissi, T., Auger, S., Drogui, P., Verma, M., and Surampalli, R.Y., 2017, Degradation of chlortetracycline in wastewater sludge by ultrasonication, Fenton oxidation, and ferro-sonication, *Ultrason. Sonochem.*, 34, 332–342.